From Miscible to Immiscible Polycarbonate/Poly(ϵ-caprolactone) Blends

Maria C. Hernández, Estrella Laredo,* and Alfredo Bello

Departamento de Física, Universidad Simón Bolívar, Caracas 1080-A, Venezuela

Patricia Carrizales, Lorena Marcano, Vittoria Balsamo, Mario Grimau, and Alejandro J. Müller

Grupo de Polímeros USB, Departamento de Ciencia de los Materiales, Universidad Simón Bolívar, Caracas 1080-A, Venezuela

Received March 25, 2002

ABSTRACT: Dielectric relaxations of polycarbonate (PC) and poly(ϵ-caprolactone) (PCL) blends that were thought to be completely homogeneous in the amorphous phase from many previous calorimetric studies are performed by using the thermally stimulated depolarization currents technique. Samples kept for 18 months at room temperature were compression-molded and then either quenched or slowly cooled. Quenched samples evidenced a phase separation for the 20/80 PC/PCL composition and the existence of continuous concentration fluctuations for other blend compositions. The slowly cooled samples from the melt exhibited an increase of the crystallinity degree for both blend components, together with a segregation of a predominantly rich PCL phase and the appearance of high-temperature relaxations attributed to interfacial polarization. These findings are confirmed by new calorimetric results on the same blends and by transmission electron microscopy. The spherulitic growth rate also points to the coexistence of two phases which are not completely immiscible but remain separated, each one being rich in one of the blend components. The phase separation of the PC/PCL blends increases with long storage times at room temperature. The driving force behind this segregation process seems to be the slow crystallization of the PCL component during storage. Once the blends have undergone phase separation, only extrusion in the melt or solution mixing can increase their miscibility.

Introduction

During the past several years, polycarbonate/poly(ϵ-caprolactone) (PC/PCL) blends have been extensively studied. Different aspects of their behavior, like miscibility, crystallization kinetics, antiplasticization, and mechanical properties, have been investigated.[1−7] This blend system is one of the few examples in which a homogeneous mixing of the components in the melt and in the amorphous phase, over the whole composition range, has been reported. Depending on composition and temperature, semicrystalline−semicrystalline, semicrystalline−amorphous, and amorphous−amorphous states are possible. To our knowledge, all previous works report the presence of only one glass transition temperature, T_g, upon cooling, since the amorphous phase seems to remain a homogeneous mixture of both polymers. Nevertheless, a controversial aspect has been the compositional variation of the glass transition. Several expressions have been used to predict its value. Cheung and Stein[4] found that the Fox equation can only accurately predict the T_g values for blends where the PC is the majority component and that the Braun−Kovacs expression should be used in the other range. However, Ketelaars et al.[8] could apply the equation over the entire composition range. On the other hand, Balsamo et al.[7] found that although the Fox equation can describe the compositional dependence of T_g, the accuracy of the fit depends on the PCL molecular weight, and better correlations were obtained for high molecular weights. It is worth noting that, in this previous study where the blends were found miscible, the DSC traces showed a progressive anomalous broadening of the heat capacity step (which represents a single glass transition) with the PCL content. This broadening of the calorimetric T_g in miscible blends has been predicted by Lodge and McLeish[9] with a model based on self-concentrations. The effective local average concentration can be estimated as well as the effective glass transition of each component in the blend. The lower T_g blend component will show segmental dynamics near that of the homopolymer, whereas the segmental dynamics of the higher T_g component is closer to the blend average. These predictions are qualitatively confirmed by NMR 2D deuteron exchange on poly(isoprene)/poly(vinylethylene) miscible blends where the components exhibit wide different mean mobilities and broad distributions near the T_g of each blend, attributed to random composition variations.[10]

For the preparation of the blends, solution and melt procedures have been used.[7,11] A comparison of the results in both cases indicates that the miscibility can be attributed to physical interactions like the possible formation of an n−π complex between the electrons of the carbonyl ester and the aromatic ring of the carbonate molecule.[12−14]

The conflicting results are not only the compositional dependence of the glass transition but also the determination of the depression of the equilibrium melting point ($T_m°$) of both components in compositions where crystallization is possible, i.e., those where the PCL is the major component. It should be emphasized that the low glass transition of the PCL enables the PC to crystallize at a rate that is much higher than PC crystallization in the presence of low molecular weight plasticizers, indicating that the PCL acts as a very effective macromolecular plasticizer.[2,4,7,15] The varied results obtained in the determination of the melting point depression have had as a consequence the report of different values for the Flory−Huggins interaction parameter χ_{12}. Values that range from −2 to −0.097 can be found in the literature.[2,12,16,17] In contrast to these results, Jonza and Porter[2] could not detect any depres-

10.1021/ma0204655 CCC: $22.00
Published on Web 08/08/2002

sion in the equilibrium melting point, concluding that χ_{12} is possibly zero or slightly positive. Other authors were not able to perform the calculation of the Flory−Huggins interaction parameter due to a nonlinear dependence of the Nishi−Wang curves,[18] suggesting that the interaction parameter can be composition dependent.[4,7]

With respect to the crystallization kinetics, Balsamo et al.[7] observed by differential scanning calorimetry (DSC) that the Avrami equation is closely obeyed by both blend components up to crystalline conversion degrees as high as 60−70%. The Avrami indices varied from 3 to 4, depending on the crystallization temperature employed. The half-time ($t_{1/2}$) for crystallization exhibited a peculiar behavior; it increased for PCL as well as for PC with increasing PC content. The increase of $t_{1/2}$ for PCL is readily understood because an increase in PC raises the glass transition of the blend with the concomitant restriction of the PCL molecular mobility. However, for PC the increase in $t_{1/2}$ is unexpected. Taking into account the works of Cheung and Stein[3,5] about the formation of intermixed lamellae in the PC/PCL system, Balsamo et al.[7] attributed the aforementioned behavior to a dilution effect of the PC due to the favorable interactions between both components, making the PC reptation to the crystallizing front difficult.

Despite the consensus between several authors with respect to the miscibility of these blends, it should be mentioned that the presence of local PCL clusters, roughly 30 Å in size, above the melting point of PCL, has been suggested, and for this reason it was proposed that the amorphous phase might not be truly homogeneous. The presence of these clusters has been attributed to solvent-induced PC crystallization. However, because of the small size of these proposed nanoheterogeneities detected by small-angle neutron scattering, the amorphous phase might still appear as homogeneous when studied thermally or mechanically.[3]

Since most studies of the amorphous regions have been performed using calorimetric techniques, the objective of this work is to provide more detailed information on the amorphous region by using dielectric relaxation techniques such as the thermally stimulated depolarization currents (TSDC) technique which is very sensitive to the molecular reorientation dynamics at different scales. Also, because of the common features of the DSC and TSDC results which both are thermally stimulated techniques, performed with similar heating rates, the results should be directly comparable. In PCL homopolymer, the local motions labeled γ and β with increasing temperature give low-intensity secondary peaks at low temperatures. These modes at temperatures below T_g, where motions of large parts of the main chain are forbidden, require smaller free volume and are caused by local motions within the main chain, i.e., type A origin according to the Heijboer classification.[19] As the temperature increases, longer segments are involved in the relaxation. The segmental motions, of cooperative origin, cause the α peak occurring near the glass transition temperature determined by DSC, which is the dielectric manifestation of the glass−rubber transition. A blend is considered as partially miscible when two α peaks are observed, and they are shifted from the homopolymer positions in temperature. This kind of nanoheterogeneous structure is observed by TSDC in poly(vinyl methyl ether) (PVME) and high molecular weight polystyrene (PS) blends.[20] Also, the broadening of the single dielectric α relaxation has been related to the existence of concentration fluctuations existing in partially miscible blends.[21,22] The increased width of the α dielectric mode indicates the existence of a T_g distribution. The effect of the miscibility degree on the secondary relaxations is scarcely reported. In homogeneous systems such as the semi-interpenetrating networks polyurethane/polycyanurate, PUR/PCN, studied by Georgoussis et al.,[21] a complex behavior of the low-temperature γ and β modes is observed which cannot be accounted for by a superposition of the homopolymers secondary relaxations. In dynamic mechanical measurements on the miscible system poly(hydroxy ether of bisphenol A)/poly(ϵ-caprolactone),[23] an effect of the miscibility is observed on the secondary β relaxation.

It has been reported that although some blend systems may appear to be miscible by using calorimetric methods where a single T_g is identified, a detailed dielectric relaxation spectroscopy study shows the presence of two α modes. For example, in the reactively blended amorphous poly(ethylene terephthalate)/poly(ethylene naphthalate) PET/PEN films, the low-temperature α mode is due to a PET-rich phase and the higher-temperature mode to a PEN-rich segregated phase.[24] Besides the effects on the primary and secondary modes, a third strong indication of the existence of miscibility is provided in the TSDC spectra of homogeneous systems by the absence of a very high-intensity peak attributed to the interfacial polarization labeled MWS or ρ mode. This mode is present in pure PUR and disappears in the homogeneous network, suggesting that the microphase separation of PUR into hard and soft segments microdomains does not occur.[21] In a study on the effect of tacticity of poly(methyl methacrylate)/poly(vinyl chloride) blends, Vanderschueren et al.[25] have demonstrated the utility of the ρ peak in determining the miscibility of a blend; the ρ peak coexists with two α modes.

In this work relaxation studies on several PC/PCL blend compositions with different thermal treatments are compared to calorimetric experiments. The morphology and crystallinity degrees are also studied by TEM and WAXS experiments, and the results are analyzed in conjunction with spherulitic growth rate determinations. The results of these complementary studies will show a more complete picture on the miscibility variations of this blend system as a function of storage time.

Experimental Section

Materials. The bisphenol A polycarbonate (PC) (Lexan HF-1110-111) and poly(ϵ-caprolactone) (PCL) homopolymers used in the present study were supplied by General Electric Co. and Aldrich Chemical Co., Inc., respectively. The number-average molecular weight ($\bar{M}_n$) and polydispersity ($\bar{M}_w/\bar{M}_n$) are 25 700 g/mol and 1.58 for PC and 97 800 g/mol and 1.58 for PCL as determined by size exclusion chromatography (SEC).

The blends were prepared by melt extrusion after previously drying the PC in a vacuum oven at 373 K for 48 h. The mixing was performed in a laboratory scale screw extruder at temperatures in the range 453−468 K in the die and 463−488 K in the barrel zone, depending on blend composition as described earlier.[7] Then, the blends were pelletized and stored in a desiccator at room temperature (296 K) for 18 months. *All the samples studied here were prepared from this 18 months aged material* (with the exception of some freshly extruded samples that were prepared for comparison purposes), and different thermal treatments were applied. Before the experi-

ments were performed, all samples were dried again in a vacuum oven at 313 K for 48 h, except for the TSDC samples which were kept in the measuring cell for several days at room temperature under high vacuum.

Samples for TSDC and WAXS experiments were compression-molded films that turn out to be very difficult to prepare because both materials presented a tendency to stick to different substrates. Best results were obtained by covering a stainless steel mold surface with polyimide films (Kapton) to facilitate demolding. The pellets were compression-molded into sheets of an approximate thickness of 0.3 mm, at 523 K for 3 min. Two types of cooling conditions were used:

(a) Quenched samples, thermal treatment A: The melted material was quenched from 523 K into a mixture of water and ice.

(b) Slowly cooled samples, thermal treatment B: The melted material is slowly cooled from 523 K to room temperature at a rate of 10 K/min in a temperature programmable press.

TSDC Experiments. TSDC experiments are performed in a cell and measuring system designed in our laboratory.[26] The two stages technique consists of a polarization step and the recording of the depolarization of the sample as the temperature is raised at a constant rate. The disk-shaped sample, 20 mm in diameter and around 300 μm thick, is located in the TSDC measuring cell between two vertical metallic disks lightly spring-loaded, which are the plates of a capacitor. During the polarization step an external field, E_p (typically 1 MV m^{-1}), is applied, the temperature, T_p, being kept constant for a polarization time t_p, typically 3 min. The polarization temperature is chosen high enough so as the species under study have a short relaxation time and will consequently orient to saturation in the electric field. The cell, previously evacuated, is filled with dry pure N_2 gas, 600 Torr, during the built-in of the polarization in order to be able to reach high polarizing fields. The following step is a quenching of the sample by rapidly immersing the cell in a liquid N_2 bath. The polarization is thus frozen in, and the field is switched off at 83 K. At this initial temperature the cell is evacuated and filled with dry He gas to act as an interchange gas. The temperature is increased at a constant rate $b_h = 0.07$ K s^{-1}, and the depolarization current is recorded with a Keathley 642 electrometer connected to the electrodes, as a function of the sample temperature. The sensitivity of our system is 10^{-16} A, and the data acquisition is fully automatic. One of the advantages of the TSDC technique is its capability to isolate a particular relaxation from its neighboring peaks by carefully choosing the polarization conditions. The overlapping of peaks located at higher temperature than the mode under study is minimized by polarizing the sample near the maximum of that peak. At this temperature the relaxation time of the peak, whose contribution has to be eliminated, is long, and the dipoles responsible for this polarization are not able to reorient in significant amount when the external field is applied. Also, by partially discharging (peak cleaning) the low-temperature side of the TSDC complex peak, the contribution of modes whose relaxation occurs at lower temperatures is minimized.

Analysis of TSDC Results. To extract the relaxation time distributions of the different modes recorded in a TSDC spectrum, the direct signal analysis (DSA) is applied. The DSA is a numerical decomposition of a complex peak into elementary Debye processes, each of them characterized by a single relaxation time, $\tau(T)$.[27,28] The method consists of finding the N elementary processes whose reorienting activation energies are equally spaced in a given energy window and whose combination best fits the whole experimental TSDC profile. The recorded TSDC current density is approximated by

$$J_D(T_j) = \sum_{i=1}^{N} \frac{P_{0i}}{\tau_i(T_j)} \exp\left(-\frac{1}{b_h}\int_{T_0}^{T_j} \frac{dT'}{\tau_i(T')}\right), \quad \text{with } j = 1, M;\ N \le M/2 \quad (1)$$

where $\tau_i(T_j)$ is the relaxation time of the ith elementary process and P_{0i} its contribution to the total polarization. The variation of the relaxation time with temperature can be either Arrhenius, adequate for low-temperature relaxations in polymers (below T_g)

$$\tau_i(T) = \tau_{0i} \exp(E_{ai}/kT) \quad (2)$$

where E_{ai} is the activation energy and τ_{0i} the preexponential factor of the ith Debye process, or Vogel−Tamman−Fulcher, VTF, which is satisfactory for relaxations occurring at temperatures around and above T_g

$$\tau_i(T) = \tau'_{0i} \exp(E_{VTFi}/k(T - T_\infty)) = A_i \exp(B_i/(T - T_\infty)) \quad (3)$$

In this case T_∞ is the critical temperature at which molecular motions in the material become infinitely slow.

The DSA method adjusts $J_D(T)$ (eq 1) to the experimental data using the Marquardt−Levenberg nonlinear least-squares fitting algorithm. The adjusted parameters are the τ_{0i}'s and the P_{0i}'s corresponding to the energy window used. The results of the fitting procedure can be summarized in an energy histogram which covers the selected energy window divided in N energy bins and whose height, $P_{0i,}$ is proportional to the area under the curve corresponding to each elementary process. The procedure has been exhaustively compared to the equivalent experimental decomposition with the thermal sampling technique.[29] When analyzing segmental relaxations, a more sophisticated program is used based on a Monte Carlo algorithm that explores randomly the parameters space in order to find the set that best fits the experimental data. The program also fits the T_∞ value when VTF relaxation times are selected.[28]

WAXS Experiments. Wide-angle X-ray scattering (WAXS) experiments were performed in a Philips automatic diffractometer by using Cu Kα Ni-filtered radiation. The spectra are recorded in an angular range $5° < 2\theta < 35°$ for quenched and slowly cooled samples. The interplanar spacings that can be observed cover the main reflections originated by crystalline PCL and PC and their amorphous halos. PCL crystallizes in the space group $P2_12_12_1$ with $a = 7.496$ Å, $b = 4.974$ Å, and $c = 17.297$ Å and gives main reflections at 2θ values of 15.64° (102), 21.40° (110), 22.05° (111), 23.70° (200), 24.3° (201), and 29.85° (210).[30] PC crystallizes in the monoclinic system with $\gamma = 84°$, $a = 12.3$ Å, $b = 10.1$ Å, and $c = 20.8$ Å.[31] The main reflections originated by PC occur at 17.2° (202), 19.4° (203), 21.5° (023), and 25.5° (223). The crystallinity degree (X_c) of each blend component was determined by a peak decomposition of the WAXS blend trace which includes the crystalline sharp peaks and the wide halos identified in the amorphous homopolymers spectrum. These degrees of crystallinity are very useful in the interpretation of the TSDC spectra as they reflect the state of the material at room temperature, which is the polarization temperature used in most of the TSDC runs reported here. The amount of amorphous phase that may be observed by TSDC should be nearly the same as that given by $(1 - X_c)$ if no constraints to its mobility exist.

Differential Scanning Calorimetry Experiments. Small disk samples were cut (13 mg) from the compression-molded sheets (for the slowly cooled 18 months aged samples) or from pellets (for freshly extruded samples) and encapsulated in aluminum pans. A Perkin-Elmer DSC7 or PYRIS-1 was used to study the thermal behavior of all compositions under an ultrahigh-purity nitrogen atmosphere. The samples were usually heated to 523 K for 3 min, and then they were cooled to 153 or 243 K at 10 K/min. Finally, they were heated from 153 or 243 K up to 523 K at 10 K/min.

Transmission Electron Microscopy Experiments. Samples of the blends were first heated in an oil bath at 523 K for 5 min. Then, they were quenched down to 317 K, the temperature at which they were isothermally crystallized for 48 h. Next, they were quenched again in a water−ice bath. It should be mentioned that all samples were wrapped in aluminum foil in order to avoid any contact of the samples with silicone oil in the bath. Pyramidal samples were then cut and stained using ruthenium tetroxide vapors for a week. Ultrathin sections (∼40 nm thick) were obtained at room temperature

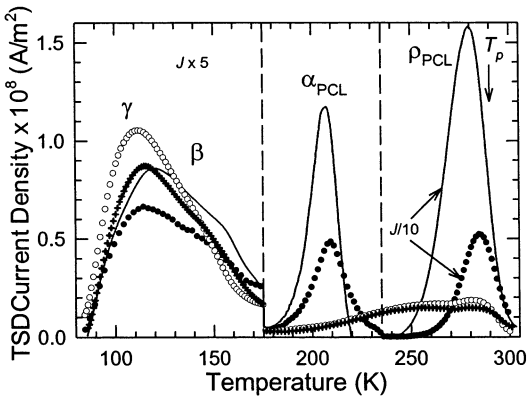

Figure 1. TSDC spectra of PCL and quenched (treatment A) PC/PCL blends, $T_p = 290$ K: (—) PCL; (●) PC/PCL 20/80; (+) PC/PCL 40/60; (○) PC/PCL 60/40.

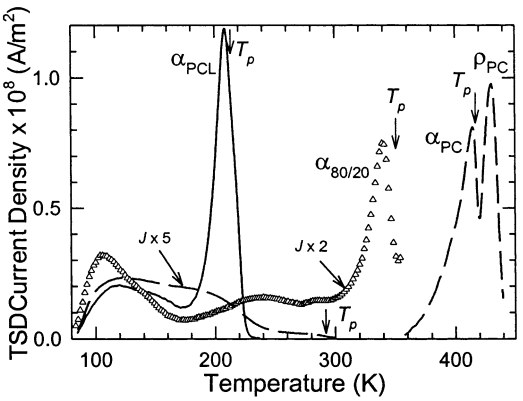

Figure 2. TSDC spectra of PC (- - -), PCL (—), and quenched (treatment A) PC/PCL 80/20 (△). The polarization temperatures are indicated by arrows. The current density is multiplied by 5 for the low-temperature part of PC and by 2 for the whole spectrum of the 80/20 PC/PCL blend.

using a Leica Ultracut UCT ultramicrotome equipped with a diamond knife. Transmission electron microscopy (TEM) was performed in the bright field mode on a JEOL JEM-1220 microscope, operating at 120 kV.

Polarized Optical Microscopy. A ZEISS MC-80 polarizing optical microscope equipped with a LINKAM-TP91 hot stage was used to investigate the superstructure formation of isothermally crystallized samples. The samples (~3 μm thick) were cut in a REICHERT-JUNG microtome at 153 K. For the experiments, the sections were held in the melt for 5 min and quenched down to the chosen crystallization temperature, T_c, which was varied from 312 to 320 K.

Results and Discussion

Dielectric Behavior of Samples with Treatment A. Figure 1 shows the TSDC spectra normalized to an electric field of 1 MV/m, between 85 and 300 K for the PC/PCL blends with thermal treatment A and neat PCL. The polarization temperature was $T_p = 290$ K. Between 85 and 175 K the low-temperature response is plotted with its intensity multiplied by 5. In this temperature range, all samples display broad multicomponent relaxations with two main distributed modes labeled γ and β, the relative contribution of each mode varying with composition and leading to significant differences in the profile of the spectrum. The observed intensities result from the composition and amount of the PCL amorphous phase in each blend and in a lesser proportion to the PC amorphous component. In the temperature interval 175 K < T < 235 K, the TSDC spectra for the PCL homopolymer and the 20/80 PC/PCL blend show a narrow α peak related to the segmental relaxation of PCL. The existence in the PC/PCL 20/80 blend of an α peak very close in temperature to the segmental relaxation of the pure PCL is an indication of the existence of a nearly pure phase of PCL. On the contrary, the 40/60 and 60/40 PC/PCL quenched blends show a broad peak over a temperature interval ranging from 190 to 300 K. These complex relaxations cover the temperature range where the glass transition of pure PCL and of homogeneous blends of increasing proportion of PC would occur. According to the Fox equation, the T_g for a 40/60 homogeneous blend should be located at 274 K and at 296 K for the 60/40 blend. The nominal composition has been corrected here to take into account the existence of crystalline phases as determined by WAXS. The extended temperature ranges covered by the relaxation of these two blends indicate the presence of a distribution of relaxation time attributed to continuous composition fluctuations as a consequence of a rather poor miscibility between blend components, in contrast with previous reports on this system that concluded the existence of a homogeneous amorphous phase.

Intense ρ peaks are observed in Figure 1 between 240 and 300 K only for PCL and the 20/80 PC/PCL blend. The temperature range $T > T_g$ and their high intensity, which is about 10 times stronger than that of the α peak, point to the interfacial origin of this relaxation. This assignment is supported by the non-ohmic character found for this peak in neat PCL at fields higher than 2.2 MV/m, while the α, β, and γ relaxations intensities still increase linearly with the applied field up to values of 4 MV/m. In PCL the ρ peak is associated with space charge accumulation at the crystal−amorphous interface.[32] By using a windowing polarization technique and analyzing the results with a general kinetic order model, we have found the distribution of depth traps present in the sample together with the variation of the kinetic order which is intermediate between a weak and strong trapping probability of free charges. The existence of an intense ρ peak only in the 20/80 PC/PCL blend, is an additional indication of the PCL segregation, in agreement with the presence of its α peak at nearly the same temperature as recorded for pure PCL. Blends with composition 40/60 and 60/40 do not show this interfacial polarization, in agreement with the existence of large and continuous concentration fluctuations which do not allow the accumulation of free charges at the interfaces of segregated phases.

In Figure 2 the TSDC spectra of the homopolymers, PC and PCL, and the 80/20 PC/PCL blend with the thermal treatment A are plotted in a wider temperature range than that used in Figure 1. The polarization temperatures (shown in the figure by arrows) are chosen to best resolve the secondary and the primary modes in each sample. The low-temperature relaxations for PC are observed between 85 and 220 K, and the intensity of the secondary modes for neat PC in this temperature interval is about 5 times weaker than that in PCL. This behavior led us to assume that the low-temperature dielectric relaxations observed in PCL-rich blends is mainly due to the reorientation of PCL molecular segments with a dipolar moment located in the amorphous regions.

The relaxations observed between 360 and 440 K for neat PC in Figure 2 are due to the glass−rubber

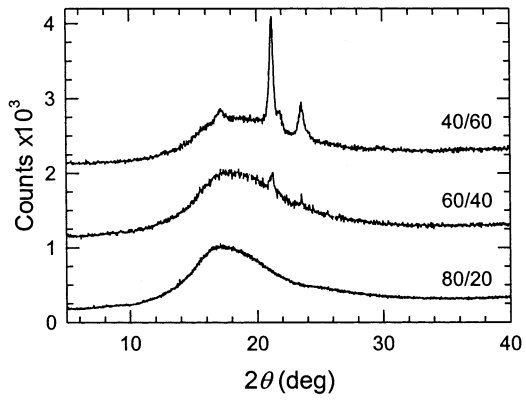

Figure 3. WAXS trace for the quenched samples of PC/PCL blends (thermal treatment A): (a) 40/60, (b) 60/40, and (c) 80/20. Curves b and a have been displaced by adding to the X-ray counts 1000 and 2000 counts, respectively.

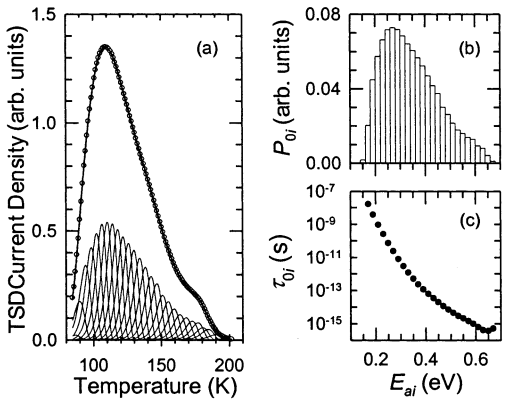

Figure 4. DSA results for the secondary relaxations of quenched PC/PCL 80/20 blend: (a) experimental data (○); (—) best fit of the data. The Debye elementary processes which sum best fits the data are also represented. (b) Energy histogram showing the contribution to the total polarization of each Debye peak. (c) Variation of the preexponential Arrhenius factor with the activation energy.

transition ($T_{M\alpha}$ = 418 K) and charge release processes ($T_{M\rho}$ = 430 K).[26] In the case of the 80/20 PC/PCL blend the WAXS trace plotted in Figure 3 shows that the material is totally amorphous. The dielectric response shows, besides a low-temperature secondary relaxation between 85 and 170 K, a broad and weak peak in the temperature interval 190−300 K, analogous to the peaks recorded in Figure 1 for the 40/60 and 60/40 PC/PCL blends. Additionally, the well-defined peak whose maximum is at 340 K is the α mode corresponding to the average 80/20 blend, close to the Fox equation prediction for this composition which gives a value of 345 K.

Let us summarize the variations in the broadening of the α relaxation with the PCL content. From Figures 1 and 2 it is seen that the α mode is narrow in the 80/20 PC/PCL blend and shows significant and equivalent broadenings for the intermediate 60/40 and 40/60 blends. For the less PC-rich blend, which is highly crystalline, the two phases are separated as there is a narrow peak close to the position of the α mode in neat PCL. The evolution of the α mode is interpreted as a progressive phase separation and miscibility reduction as the PCL component grows and the crystallinity of the material increases. Because of the similarity of the DSC and TSDC techniques, one would expect, according to the Lodge and McLeish model,[9] an increasing broadening of the α mode with PCL content which would be indicative of the existence of dynamic heterogeneities in homogeneous blends. In our case, the broadening is only observed for the two richest PC blends, and the explanation through the increment of the composition heterogeneities caused by the continuous phase separation induced by the presence of crystalline PCL and PC regions seems more sound.

The secondary relaxations profile of the 80/20 PC/PCL blend presented in Figure 2 is different from that of neat PC or PCL with a marked depletion of the higher temperature contributions, indicating that the local relaxation processes are again affected at this composition, where the existence of a narrow α peak at intermediate temperatures is proof of the homogeneous mixture of at least part of the PCL component. However, the broad and weak relaxation at intermediate temperatures, between 190 and 300 K, is evidence for some concentration fluctuations around the pure PCL component. The 80/20 PC/PCL blend is the only composition where there is a narrow α peak at the temperature corresponding to the blend composition according to the Fox equation.[33] However, its intensity is about half that of the PC and PCL homopolymers. Crystallinity is not responsible for this weak intensity as the blend is 100% amorphous as shown on the WAXS trace of the blends quenched from 523 K (thermal treatment A) shown in Figure 3. A high number of dipolar entities do not relax as a homogeneous phase; a number of dipoles realize their segmental relaxation in phases rich in either PCL or PC. These concentration fluctuations around PCL are observed as the broad peak at intermediate temperatures. The presence of a peak at higher temperatures (which would indicate the presence of a PC-rich phase) could not be detected as the sample becomes soft after undergoing the glass rubber transition of the blend at 340 K.

Relaxation Time Distribution of A Blends. To study the effect of blend composition on the secondary relaxations mainly originated by local reorientations of PCL dipoles, the relaxation time distribution is extracted by analyzing the TSDC profile, obtained after polarizing the sample at 175 K, with the DSA computer procedure.[27] The variations of the Arrhenius preexponential factors (τ_{0i}) and activation energies (E_{0i}) are found for the N Debye processes whose sum best fits the experimental curve. The results of a typical DSA analysis are presented in Figure 4 for the 80/20 PC/PCL blend. The experimental curve is normalized to a unit polarization in order to compare the magnitude of the sum of the squared residuals, χ^2, for different samples. The complex broad relaxation is numerically decomposed in 27 elementary Debye processes whose energy varies between 0.15 and 0.67 eV. The preexponential factors vary between 10^{-7} and 10^{-16} s, and a $\chi^2 = 2 \times 10^{-10}$ is calculated. In Figure 4a the experimental data (open circles) and the best fit (continuous line) are plotted. In Figure 4b the activation energies histogram is presented, the height of each bar being representative of the contribution of this Debye process to the total polarization, and in Figure 4c the variation with the activation energy of the preexponential factor is drawn. It is to be noted that on the high-temperature tail of the global peak the values of $\tau_{0i}(E_{0i})$ are low, i.e., correspond to activation entropies of 4.8×10^{-4} eV/K. This is always found, either experimentally with the thermal sampling technique[34] or with the DSA decom-

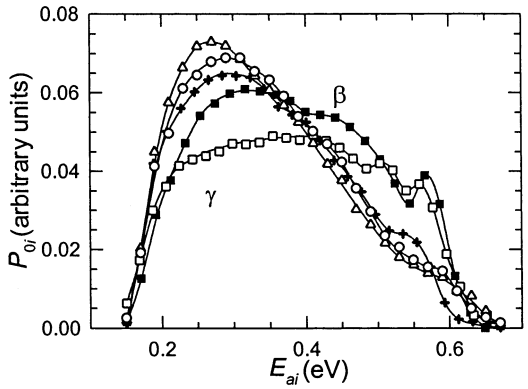

Figure 5. Comparison of the energy histograms obtained from DSA procedure for the PC/PCL quenched blends: (■) PC/PCL 0/100; (+) PC/PCL 40/60; (○) PC/PCL 60/40; (△) PC/PCL 80/20; (□) PC/PCL 100/0. The lines are drawn to guide the eye.

position, when the rise of the α peak overlaps the decrease of the β peak as is the case here. The DSA results obtained for the quenched blends and homopolymers show a similar energy interval and $\tau_{0i}(E_{0i})$ dependence. However, the observed variations in profiles of the secondary relaxations (see Figures 1 and 2) affect the distribution of activation energies, promoting the lower energy processes and lowering the contribution of the higher ones, as the PCL proportion in the blend is lower. In Figure 5 the contribution, P_{0i}, of each Debye process identified by its activation Arrhenius energy, E_{ai}, to the total polarization (normalized to a unit value) is represented for the homopolymers and three blends with thermal treatment A. It is readily seen that the higher temperature processes present in both homopolymers are depleted in the blends, and the γ process is favored. This effect is larger in the PC/PCL 80/20 blend, which is the only one in this series to show a degree of miscibility as detected by a narrow α peak at a temperature corresponding to the nominal blend composition.

After observing by TSDC that the miscibility of the blends did not seem to be total as previously gathered by DSC for freshly extruded or solvent-cast samples,[7] it was decided to prepare slowly cooled samples in order to investigate the effect of enhanced crystallinity by both DSC and TSDC. Therefore, the slowly cooled samples from the 18 months aged pellets (thermal treatment B) were prepared (see Experimental Section).

Thermal Behavior of Blends with Treatment B. Figure 6a,b presents a series of heating DSC scans performed at 10 K/min for the slowly cooled samples (with thermal treatment B). Two heat capacity, ΔC_p, steps identified as T_g's are observed, except for the 80/20 PC/PCL blend, indicating that the blends have phase separated in general agreement with the TSDC results for slowly cooled samples to be presented below. The two T_g's correspond to a PCL-rich phase and a PC-rich phase since their values do not correspond to those of the homopolymers but are slightly shifted to intermediate values. Simultaneously, an endotherm corresponding to the melting process of the PCL can be observed up to PCL contents of 60%.

Table 1 lists the relevant thermal transitions and enthalpies that can be extracted from the data of Figure 6. The T_g of neat PCL is observed at 205 K, a value that is in agreement with that measured by TSDC, 207 K. In the case of the blends, a low-temperature T_g corresponding to a PCL-rich phase is observed at increasingly

Table 1. Thermal Behavior of Slowly Cooled PC/PCL Blends (Thermal Treatment B)[a]

	PC	PCL					
blend	T_g (K)	T_g (K)	T_{cp} (K)	ΔH_c (J/g)	T_m (K)	ΔH_m (J/g)	T_{gFOX} (K)
0/100							
cooling			303.9	77			
heating		205			328.2	80	205
5/95							
cooling			300.3	52			
heating		206			330.3	60	214
10/90							
cooling			299.1	74			
heating	399	207			329.5	67	227
15/85							
cooling			300.1	80			
heating	356	208			328.8	71	262
20/80							
cooling			299.8	68			
heating	398	209			330.2	57	246
30/70							
cooling			299.8	66			
heating	378	209			330.2	56	265
40/60							
cooling			299.3	56			
heating	390	212			331.2	52	280
100/0							
cooling							
heating	416						416

[a] T_g was measured as the midpoint value of the heat capacity step during the heating scan. T_{cp} is the peak crystallization temperature measured during the cooling scan. ΔH_c is the enthalpy of crystallization and ΔH_m the enthalpy of fusion. T_m is the peak melting temperature measured during the heating scan. T_{gFOX} is the value of the T_g predicted by the Fox equation after taking into account the composition of the amorphous phase for the PCL component.

higher temperatures as the PC content is increased up to 40%. Quantitatively, the shift in T_g is only 7 K with respect to pure PCL (from 205 to 212 K). In the case of neat PC, Figure 6b and Table 1 show that the T_g is located at 416 K, again in good agreement with the TSDC measurements for neat PC, 418 K. A lower T_g was observed for the PC-rich phase of the blends ranging from 356 to 399 K as the blend composition varies. Nevertheless, there is no regular trend of the T_g value with the amount of PCL in the blend.

The Fox equation, as mentioned above, can be used to calculate the T_g values of fully miscible amorphous blends as a function of composition:[33]

$$\frac{1}{T_{gFOX}} = \frac{w_1}{T_{g1}} + \frac{w_2}{T_{g2}} \tag{4}$$

where T_{gFOX} is the blend glass transition and T_{gi} and w_i are the glass transition and weight fraction of each amorphous component, respectively. If the equation is applied with the experimental T_g values of neat PCL and PC, the values for the T_{gFOX} of miscible blends are obtained as a function of composition. For this calculation we corrected the composition by subtracting only the crystalline part of the PCL using the crystallization enthalpy (ΔH_c) obtained for this component. However, even with this correction, an error is involved since the experimentally determined T_g value for neat PCL corresponds to a semicrystalline polymer and not to an amorphous one; it should be remembered that PC and PCL can only be miscible in the amorphous state. Table 1 lists the values of the T_{gFOX} predicted by the Fox equation for the slowly cooled samples if the blends

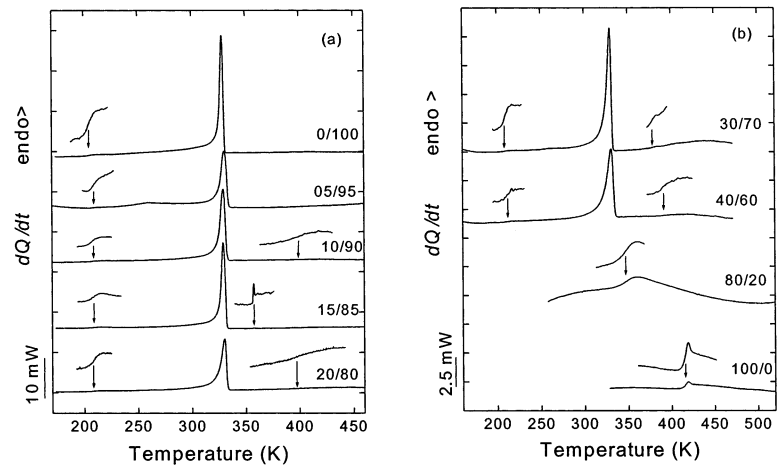

Figure 6. DSC heating scans of slowly cooled PC/PCL blends at 10 K/min (thermal treatment B, blend composition is indicated as a legend).

Table 2. Blend Compositions Estimated from T_g Values by the Fox Equation (See Text)

PC/PCL blend	PC-rich blend		PCL-rich blend	
	% PC	% PCL	% PC	% PCL
0/100			0.0	100.0
5/95			1.0	99.0
10/90	95.9	4.1	2.1	97.9
15/85	83.7	6.3	3.5	96.5
20/80	95.6	4.4	3.8	96.2
30/70	90.4	9.6	3.6	96.4
40/60	93.5	6.5	6.6	93.4

under consideration were fully miscible in the amorphous phase. However, the PC/PCL blends investigated in this work are only partially miscible as demonstrated above. To have an idea of the phase composition, if we suppose that there are no more phases present, the Fox equation can be used to calculate the composition of the amorphous phases using the experimental values reported in Table 1 for the PC- and the PCL-rich phases.

Table 2 lists the calculated composition weight fractions in each amorphous phase, rich in either PC or PCL, from the Fox equation, using the T_g's given in Table 1. In the case of the PCL-rich phase, it seems that the incorporation of PC in this phase is marginal and increases slightly (from 1 to 6.6% PC) upon increasing the PC weight fraction. In the case of the PC-rich phase, the incorporation of PCL is also small, and it does not show a specific trend.

Isothermal spherulitic growth experiments to be presented below indicate that the spherulitic growth rate of the PCL phase is affected by the amount of PC in the blend in proportions, which would indicate much higher contents than those suggested in Table 2. The results of Table 2 might be interpreted by arguing that other phases not detected by the DSC might be present, including a miscible phase with a higher PC content. In fact, the TSDC results for the quenched 40/60 and 60/40 PC/PCL blends presented in the above section show a complex phase structure with concentration fluctuations indicated by very broad α relaxations; the relaxation spectra of the slowly cooled blends to be presented below exhibit a higher degree of phase separation with α relaxations that are still wider than in the neat PCL.

The behavior of the slowly cooled blends (with thermal treatment B) is noteworthy since it has been reported extensively that PC/PCL blends are supposed to be miscible in the amorphous phase for the entire composition range.[1−7] Previous studies have indicated that the system has a lower critical solution temperature (LCST) located at around 533 K.[1,12] Therefore, if this phase diagram is taken to be valid for the blends prepared here, it would be expected that holding the samples in the melt at 523 K would cause mixing if the 5 min annealing time is enough for equilibrium to be established. However, in view of the above-mentioned results, we gather that this is not the case. Other thermal treatments were performed to try to enhance the samples miscibility. For instance, longer times at 523 K were employed (15 and 30 min), but still the results were nearly identical to those of Figure 6. It would seem that the storage of samples at room temperature for 18 months induced a phase separation process that is very difficult to reverse. The reason for this apparently irreversible behavior could be the hindered diffusion of PC chains once they have been phase segregated. The slow process of phase segregation at room temperature may be originated in the additional crystallization of the PCL component or PCL-rich phase during storage because those blends with an excess of PCL will have T_g values below room temperature (see Table 1).

At this point a small amount of new blend samples was extruded to corroborate the previous DSC results of ref 7 about blend miscibility; these will be referred to as "freshly extruded" samples. Figure 7a shows DSC heating scans of the 18 months old sample, and Figure 7b shows a freshly extruded 15/85 PC/PCL blend after storage at room temperature and after cooling from the melt at 10 K/min (i.e., the second heating run in Figure 7a is nearly equivalent to that of the slowly cooled samples in Figure 6). Both sets of samples were dried in a vacuum oven for 48 h at 313 K before loading them in the DSC and cooling them to 243 K, and then the first heating was started. It is clearly seen that the freshly extruded samples (Figure 7b) do not exhibit any detectable high-temperature T_g that could be indicative of the presence of a PC-rich phase of similar composition to that present in the 18 months aged samples (Figure 7a).

Table 3 compares crystallization and melting data for the PCL component of samples that were aged 18 months with freshly extruded samples; these data were extracted from Figure 7. It should be mentioned that both kinds of samples were analyzed through SEC to see whether some degradation or chemical change could

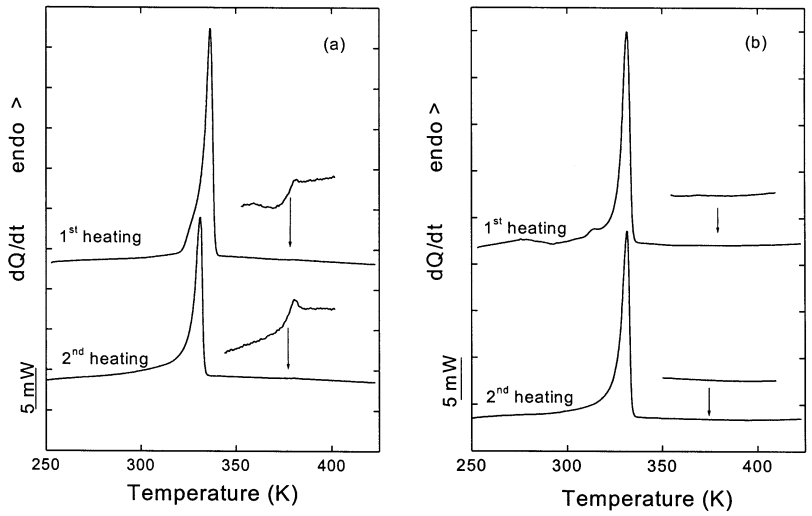

Figure 7. DSC heating scans: (a) 18 months aged 15/85 PC/PCL blend; (b) freshly extruded 15/85 PC/PCL blend. Thermal treatment is described in the text.

Table 3. Thermal Data Extracted from Figure 7 from Aged and Freshly Extruded PC/PCL Blends (See Text)

	aged 18 months at 298 °C				freshly extruded			
PC/PCL	T_c (K)	ΔH_c (J/g)	T_m (K)	ΔH_m (J/g)	T_c (K)	ΔH_c (J/g)	T_m (K)	ΔH_m (J/g)
0/100								
first heating			336.9	95			331.7	74
cooling	304.7	72			301.9	68		
second heating			331.9	80			332.4	77
15/85								
first heating			336.6	99			331.7	82
cooling	301.2	70			299.2	70		
second heating			331.4	80			331.7	72
40/60								
first heating			340.2	87			328.4	47
cooling	296.7	44			273.7	27		
second heating			327.9	56			321.7	36

be the reason for the obtained results. Nevertheless, no changes were detected.

The data corresponding to the first heating in Figure 7 contain information about the thermal history of the samples that includes their preparation by melt extrusion, aging time at room temperature, and drying time at 313 K. When the data for neat PCL are examined in Table 3, it is clear that the PCL that was aged 18 months exhibits a higher enthalpy of fusion during the first heating run as compared to the freshly extruded one (95 vs 74 J/g, see Table 3) as a result of slow crystallization at 298 K during storage (it must be remembered that the T_g of PCL is at around 205 K, so crystallization at 298 K is commonly observed during storage); the same holds for the PCL component of the blends. The melting point is also higher for the first heating run of the aged PCL or PCL components, in agreement with longer crystallization time or annealing. However, in the second heating scans similar results are obtained for neat aged and freshly extruded PCL as would be expected after erasing the thermal history of the neat homopolymer sample.

Perhaps the most interesting results in Table 3 are those obtained for the 40/60 PC/PCL blend. In this case, let us compare the first heating runs of the freshly extruded with the 18 months aged sample. The freshly extruded and therefore more miscible 40/60 PC/PCL blend presents a much lower degree of crystallinity according to its value of enthalpy of fusion (47 J/g) as compared to the less miscible and phase-separated 18 months aged sample (87 J/g). Additionally, the melting point of the freshly extruded 40/60 PC/PCL sample is 328.4 K, a value much lower than that corresponding to the 18 months old sample (340.2 K). When the second heating results in Table 3 (equivalent to the slow cooling conditions or thermal treatment B) are compared for the 40/60 PC/PCL blends, there is still a big difference between the freshly extruded sample and the 18 months aged sample in both the melting point and the melting enthalpy values, both values being higher for the 18 months aged sample.

The results presented above support the already mentioned hypothesis that the blends are close to being fully miscible when they are freshly prepared[7] but tend to phase separate during storage at 298 K for long periods of time, a fact related to the ability of the PCL component to crystallize during this time. To the best of our knowledge, only Stein et al.[3] have suggested that the amorphous phase above the melting point of PCL might not be truly homogeneous due to presence of local clusters of about 30 Å that were not detectable by DSC and DMA.

Once the blends were aged for 18 months and phase separated, we were not able to mix them again by thermally treating them as already mentioned above. However, if the aged samples are dissolved in a common solvent (like dichloromethane) and then reprecipitated, a miscible sample with only one T_g as detected by DSC can be obtained.

Dielectric Behavior of Blends with Treatment B. Figure 8 shows the TSDC spectra for the slowly cooled blend compositions (treated with the thermal protocol B) in order to compare with the DSC results discussed above. As in Figure 1, there are three temperature regions clearly differentiated: between 85 and 175 K the secondary relaxations zone; the temperature interval 175 K < T < 235 K, where all blends show a peak near the T_g of PCL homopolymer at 207 K; the high-temperature region 235 K < T < 305 K characterized by an intense peak for all blend compositions. All samples were polarized at a $T_p = 290$ K and normalized to 1 MV/m; as a comparison, the spectrum of PCL is also included.

The relaxations observed in the low-temperature region of Figure 8 are as in Figure 1 complex and broad, composed by two distributed modes, γ and β. Neverthe-

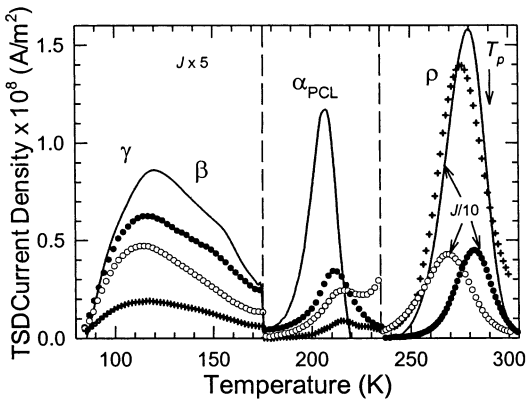

Figure 8. TSDC spectra of annealed (treatment B) PC/PCL blends, $T_p = 290$ K: (—) PCL; (●) PC/PCL 20/80; (+) PC/PCL 40/60; (○) PC/PCL 60/40.

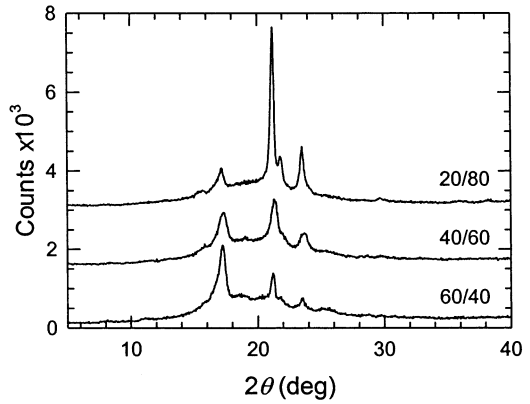

Figure 9. WAXS trace for the annealed samples of PC/PCL blends (treatment B): (a) 20/80, (b) 40/60, and (c) 60/40. Curves b and a have been displaced by adding to the X-ray counts 1000 and 2000 counts, respectively.

less, the curves profile appears to be the same at different compositions and very similar to that of neat PCL. The intensity variation of the spectra is associated with blend composition together with changes in the amount of crystalline phase of PCL with thermal history. It is worth noting that the low-temperature relaxations of the slowly cooled 20/80 PC/PCL blend in Figure 8 are almost the same as in Figure 1 for the equivalent quenched sample and thus independent of the thermal treatment applied.

The WAXS traces for the blends with thermal treatment B are shown in Figure 9. The slowly cooled samples show the crystallization of both the PCL and the PC phase, the degree of crystallinity of the PCL phase increasing with its amount in the blend from 29% in the 60/40 PC/PCL blend to 48% in the 20/80 compound. The crystallinity degrees calculated for the blends whose WAXS trace is reported in Figure 3 (blends with thermal treatment A) and Figure 9 (blends with thermal treatment B) are reported in Figure 10 as a function of the PCL content. The plasticization effect of PCL on PC in the slowly cooled samples is evident as the PC crystallizes. The degree of crystallinity of PC peaks at a value of 22% for the 40/60 PC/PCL blend. The PCL crystallinity curve shows that for the 20/80 PC/PCL blend there is no difference between the A and B treated samples. This similarity is also found on the TSDC low-temperature spectra shown in Figures 1 and 8. Both components in the slowly cooled samples for blend compositions 40/60 and 60/40 are

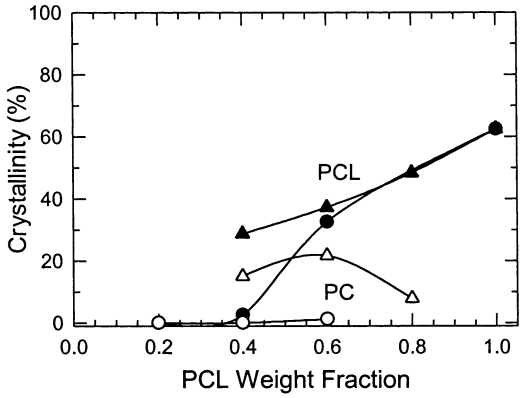

Figure 10. Degree of crystallinity, X_c, variation for PC and PCL components as a function of the PCL weight fraction obtained from the WAXS experiments: (●) X_c of PCL in quenched samples; (○) X_c of PC in quenched samples; (▲) X_c of PCL in annealed samples; (△) X_c of PC in annealed samples.

more crystalline than in the quenched sample, showing that the increase of ordered regions promotes a better phase segregation.

The relaxations observed in the TSDC spectra of the slowly cooled samples, represented in Figure 8, in the temperature range 175 K < T < 235 K for all blends, are associated with the glass−rubber transition of a rich PCL phase as the corresponding α peaks are only slightly displaced on the temperature axis from the PCL homopolymer position. Comparing the effect of thermal history at the same composition (Figures 1 and 8), it is evident that the controlled cooling promoted phase separation for blend compositions PC/PCL 40/60 and 60/40, which were considered as partially homogeneous after thermal treatment A. The 20/80 PC/PCL blend, already heterogeneous after quenching, is unaffected by the controlled slow cooling. Moreover, in agreement with the idea of an heterogeneous system deduced from the appearance of an α peak characteristic of a PCL predominant phase (see Figure 8), the temperature interval between 235 and 305 K shows a very intense ρ peak for all blend compositions probably produced by charge trapping at the interfaces existing in these heterogeneous blends. The non-ohmic character of the ρ peak present in neat PCL and in the nonmiscible blends has been checked in the 60/40 PC/PCL blend; it was found that for applied fields higher than 4 MV/m the intensity of the ρ peak saturates while the γ, β, and α modes intensity are still increasing linearly up to 7.2 MV/m. When the α peaks are properly isolated by polarizing the samples near the maximum, $T_p \approx T_{M\alpha}$, to minimize the influence of the ρ peak located at higher temperatures, the α relaxations show a weak shift toward high temperatures as the PCL content decreases, from pure PCL to the 60/40 PC/PCL blend. This weak shift would indicate that the amount of PC within the PCL-rich phase increases as the proportion of PC in the blend increases. A similar result was obtained by DSC as explained above (see Table 2).

Relaxation Time Distribution of Blends with Treatment B. To study the effect of phase segregation on the local relaxations, the DSA analysis of low-temperature spectra obtained in the same conditions as previously described is performed. The distributions in τ_{0i} and E_{ai} are extracted, and the results for different blend compositions are compared. The activation energy range for the best fit remains between 0.15 and 0.67 eV, and the corresponding preexponential factor varies

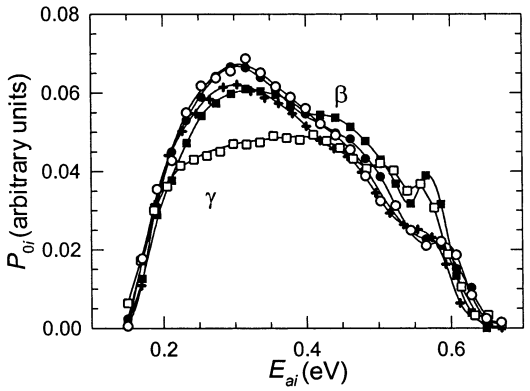

Figure 11. Comparison of the energy histograms obtained from DSA procedure for the PC/PCL annealed blends: (■) PC/PCL 0/100; (●) PC/PCL 20/80; (+) PC/PCL 40/60; (○) PC/PCL 60/40; (□) PC/PCL 100/0. The lines are drawn to guide the eye.

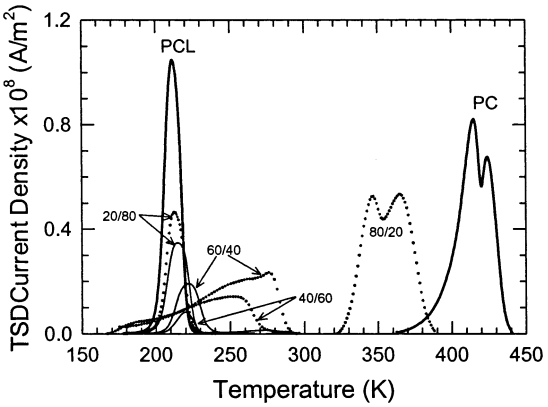

Figure 12. α modes after partial discharge up to $T_{M\alpha}$ −10 K for PC and PCL homopolymers (thick lines) and PC/PCL blends (···) quenched samples (thin lines) slowly cooled samples.

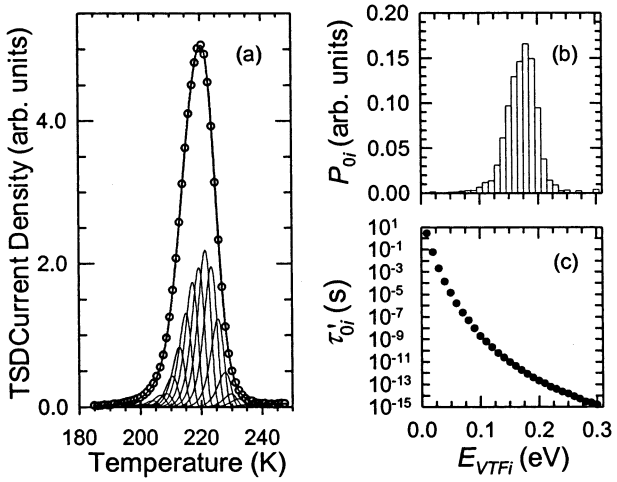

Figure 13. SADSA results for the primary relaxation of PC/PCL 40/60 slowly cooled blend: (a) experimental data (○); (—) best fit of the data; the Debye elementary processes which sum best fits the data are also drawn. (b) Energy histogram showing the contribution to the total polarization of each Debye peak. (c) Variation of the preexponential VTF factor with the activation energy.

between 10^{-7} and 10^{-16} s, in a similar way as that observed for the blends treated with thermal protocol A. The effect of blend composition on the local relaxations as the material is phase separated is observed as a smooth variation of the energy histogram shown in Figure 11. The effect of larger phase segregation than before should affect the energy landscape associated with the local reorientation of dipolar segments; this is translated by the energy histograms representing the relative contribution to the total polarization of each elementary process. When the PCL phase is segregated as in the slowly cooled samples, the different samples have a low-temperature secondary relaxation spectra that reproduces well that of the neat PCL. The molecular local dynamics are not significantly modified when the phases are segregated as opposed to the results observed for the quenched samples in which partial miscibility was detected. In this case, the large composition fluctuations, evidenced by the broad α peaks, are sufficient to affect the energy landscape felt by the dipolar molecular segments. Although the blending effect on secondary modes has not been exhaustively studied, as it is generally believed that the effect on the short-range motions is not significant,[35] it has been shown[21,23] that in some miscible systems the profile and position of the secondary modes vary, thus indicating a strong interaction between blend components. The changes observed in the energy histograms presented in Figures 5 and 11 again confirm the existence of interactions at a local scale when miscibility is present. In Figure 5 the histogram that differs the most from that of the homopolymers is the 80/20 blend, which is the best mixed one at a molecular level.

In Figure 12 the "clean" α relaxations recorded for all blend compositions, with thermal treatments A and B, together with the neat homopolymers are represented to summarize the TSDC peaks that are the dielectric manifestation of the glass−rubber transition. These clean peaks have been partially discharged to a temperature of T_M −10 K in order to minimize the Arrhenius contributions of the secondary relaxations located at lower temperatures. One can observe the very significant differences between the quenched (symbols) and the slowly cooled samples (thin lines). The traces due to the latter samples are easily interpreted as resulting from partially miscible blends where the primary relaxation corresponding to the PCL-rich phase is very near that of neat PCL, the temperature of the peak maximum shifting gradually to higher temperatures, as the PC content increases; the observed shift of the clean α peak is 13 K on going from neat PCL to the 60/40 PC/PCL blend with treatment B. This shift allows an estimate of the PC presence in the PCL amorphous phase of the blend with a 60/40 nominal composition, which amounts to 10% if the $T_{M\alpha}$'s are used in the Fox equation. The detailed analysis with the SADSA procedure gave the fitted curve plotted in Figure 13a for the slowly cooled 40/60 PC/PCL blend. Each Debye peak contributes P_{0i} to the total polarization, giving the energy histogram represented in Figure 13b. The preexponential factor, τ'_{0i}, of the VTF relaxation time of each Debye process is represented as a function of E_{VTFi} in Figure 13c. The distribution is nearly Gaussian, and the mean energy is 0.18 eV with a mean value of 10^{-12} s for τ'_{0i}. The use of VTF relaxation times for the decomposition of the α mode deserves some justification. As the peaks have been partially discharged by the cleaning procedure to $T_{M\alpha}$ − 10 K, the Arrhenius contributions on the low-temperature side are minimized as seen by the shift of the α peak to higher temperatures. Additionally, one can observe in the energy histogram presented in Figure 13b,c that the low-energy elementary modes have a very low contribution to the total polarization. Another alternative is to

analyze the α mode with Arrhenius relaxation times which is the usual choice made when performing the experimental thermal sampling and which leads to inconsistencies such as very small preexponential factors, together with very high activation energies of several electronvolts. An exhaustive comparison of the experimental and the numeric decomposition has been made in a previous work on the PCL homopolymer.[29] Our result, even if the distribution is somewhat truncated by the partial discharge, appears to be a better description of the molecular relaxation parameters which define the α mode.

The results obtained for the other blend compositions are comparable with a very slight increase in the VTF energy. The value of the T_∞ which is characteristic of each material is 152.5 K for PCL and for the 20/80 PC/PCL blend and increases from 154.5 to 160.5 K for the 40/60 and the 60/40 compositions, respectively. This increase in T_∞ follows the small $T_{M\alpha}$ shift of the segmental modes observed in Figure 12. In this same figure the diversity of results obtained on samples with treatment A for the segmental mode is shown, from the 20/80 PC/PCL blend, which is very similar to the neat PCL α mode, to the broad relaxations obtained for the 40/60 and 60/40 PC/PCL blends. These differences indicate the increase of the miscibility as the PCL concentration and crystallinity decrease until a unique well-defined mode is recorded for the 80/20 blend at a temperature which is close to that calculated from the Fox equation for the nominal composition of this blend.

From this same Figure 12, the variation of the areas under the curves of the α modes can be studied and compared to the corresponding areas recorded for the secondary transitions. If it is assumed that the secondary transitions are the least affected by the blending process, then the area under the low-temperature curves shown in Figures 1, 2, and 8 could be assumed as representative of the amount of mobile amorphous phase present in the blends. A plot of the area under the primary transitions as a function of the area under the secondary transitions should fall on the straight line drawn from the origin to the point defined by neat PCL if the proportion of mobile amorphous phase is constant. It is found that all the immiscible blends fall below this line, showing that an important part of the amorphous chains is not undergoing the cooperative motion that originates the segmental mode. Additionally, the 40/60 blend shows more constraints than the other materials, in both the local and cooperative modes, as can be seen by the low intensity of the TSDC trace for this composition in Figure 8. This is the material that has the highest PC crystallinity (see Figure 10), and the lowest amount of mobile phase seems to be related to the existence of PC lamellae which might trap amorphous PCL at the crystallization step; these chains remain rigid due to the constrains applied by the neighboring PC crystal lamellae and do not contribute to either the local or segmental dynamics which occur in the polarization stage of the sample. Cheung et al.[5] have studied the amorphous phase thickness at 75 °C, where the PCL is in the molten state, and shown that its invariance at high PCL concentrations with blend composition indicates the rejection of PCL from the interlamellar PC regions. At lower PCL contents the amorphous PCL zones are incorporated or trapped within the interlamellar regions, resulting in major constraints on the molecular motions. If fewer PCL dipoles located in the amorphous phase are able to orient, the intensity of the corresponding TSDC peak will be lower as the peak area is proportional to the number of reorienting dipolar segments times the squared mean dipolar moment. As our 40/60 PC/PCL blend is a semicrystalline−semicrystalline blend, the amorphous PCL phase would still be in the composition range of the semicrystalline−amorphous blend reported by Cheung et al.[5] as that where the amorphous PCL inclusions are incorporated within the PC lamellae. The constraints will here be originated by both the PC and PCL lamellae.

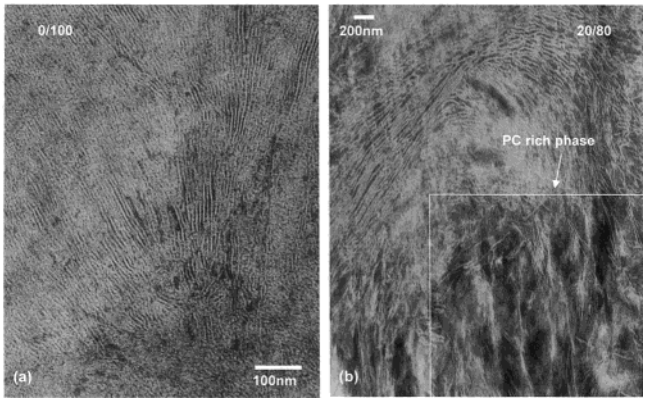

Figure 14. TEM micrographs: (a) neat PCL; (b) 18 months aged 20/80 PC/PCL blend.

Phase Segregation Observed by TEM. With the purpose of obtaining further evidence of phase segregation in the 18 months aged PC/PCL samples, they were isothermally crystallized at 317 K for 48 h (see Experimental Section). The isothermal crystallization at a relatively high temperature for a long time is designed to produce thicker lamellae so that they could be easily observed by TEM.

Figure 14a shows a TEM micrograph of neat PCL isothermally crystallized as indicated above. This micrograph shows that 1 week exposure time to RuO_4 is effective in staining the amorphous regions of PCL, in agreement with the results of Huong et al.[36] The white patterns are the PCL lamellae, and the mean lamellar thickness was directly measured in several micrographs. A mean value of 50 Å with a standard deviation of 15% was obtained. This value is somewhat lower than those measured previously by small-angle X-ray scattering (85−90 Å),[37,38] but it may be due to the staining technique employed here, since for instance in polyethylene it has been reported that staining yields lower lamellar thickness when compared to etching followed by carbon replication.[39]

Figure 14b shows a micrograph of a 20/80 PC/PCL. DSC measurements on this isothermally crystallized sample indicated that the PCL component developed a high crystalline content (80%) while the PC only crystallized 15%, which is to be expected due to the long crystallization time at 317 K. The micrograph corresponds to a sample that seems to have been phase separated in the melt; otherwise, the PCL-rich regions (with a high population of very long lamellae) would not be isolated. The lamellae in these PCL-rich regions are thinner than in neat PCL with a mean lamellar thickness of 32 ± 4 Å.The rectangular region indicated in Figure 14b by the arrow is probably a PC-rich region where a much lower number of lamellae are observed, indicating a lower crystallinity as expected in such

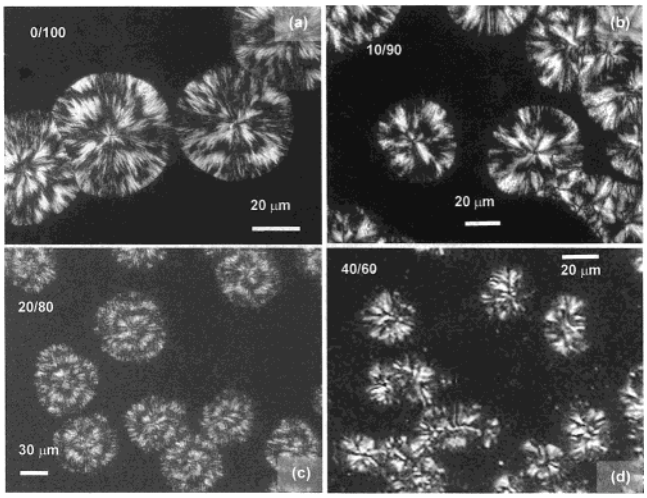

Figure 15. Polarized optical micrographs for neat PCL and selected 18 months aged PC/PCL blends of the indicated compositions during isothermal crystallization at 320.2 K.

regions. Even the lamellae observed are thinner and shorter and they might also correspond to PC lamellae since only 15% of the PC chains crystallize in this sample according to DSC measurements.

Spherulitic Growth of the PCL Component in PC/PCL Blends. The isothermal crystallization of neat PCL and of the PCL component in the PC/PCL blends was followed by polarized optical microscopy, and some examples of the superstructures obtained are provided in Figure 15 for samples isothermally crystallized at 320.2 K. These samples correspond to 18 months aged blends.

Neat PCL exhibits in Figure 15a well-developed spherulites with a rather complex extinction pattern that consists of two features: a Maltese cross and irregular banding that seems to interfere with the regularity of the Maltese cross. When 10% PC is added, the morphology of the PCL spherulites does not seem to vary much (see Figure 15b). However, when the 20/80 PC/PCL sample was crystallized at 320.2 K, the PCL spherulites suffered some morphological changes evidenced in Figure 15c. The banding is now more regular and the contour of the spherulites slightly less regular; they are not perfect circles anymore (compare with Figure 15a). The appearance of more regular or clearer banding in PCL crystallized in blends as compared to neat PCL seems to be a general feature since it has been observed for other blends like poly(styrene−acrylonitrile)/PCL[40,41] and poly(vinyl chloride)/PCL.[42,43]

The PCL spherulites grown in the melt of the 40/60 PC/PCL blend are highly irregular with no discernible Maltese cross and noncircular borders, as seen in Figure 15d. These superstructures could also be axialites or bidimensional arrays of lamellae since they do not seem to have three-dimensional symmetry. Ong and Price[43] have found for PVC/PCL blends that are reported to be miscible, similar deformity in PCL spherulites for samples with high PVC content. The shape irregularity might be due to interference of the PC-rich phase that could be located in the intraspherulitic amorphous regions and might also be rejected to the surroundings of the growing superstructure.

The morphological features of the PCL spherulites presented in Figure 15 indicate that, despite partial phase separation, there are definite interactions with PC; otherwise, they would not be that much altered by

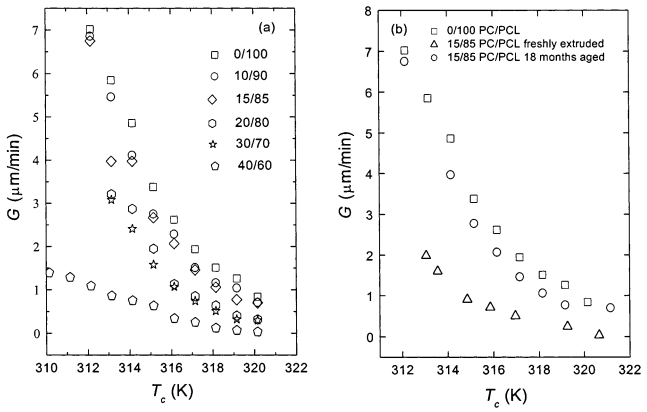

Figure 16. Spherulitic growth rate as a function of isothermal crystallization temperature: (a) 18 months aged PC/PCL blends of the indicated composition; (b) comparison of spherulitic growth kinetics of an 18 months aged 15/85 PC/PCL blend and a freshly extruded blend of identical composition.

PC addition. Again, in this case, the evidence suggests that if the blends are separated they are not completely immiscible but remain in two coexisting phases, each one being rich in one of the blend components.

Figure 16a presents spherulitic growth rate data for all the 18 months aged samples that display PCL spherulites. Even though the exact composition of the PCL-rich phase is not known, it is clear that as the PC content in the blends is increased, the spherulitic growth rate decreases as one would expect on the basis of the more rigid chemical structure of PC as compared to PCL.

It is difficult to estimate what the growth rate would be if the blends would be fully miscible. For this reason a freshly extruded sample was isothermally crystallized and compared to an 18 months aged sample of identical composition, i.e., 15/85 PC/PCL. The results can be seen in Figure 16b where the freshly extruded sample is displaying a slower crystallization rate in view of its increased miscibility with PC.

Conclusions

We have shown that PC/PCL blends that were regarded as a fully miscible system in the amorphous state exhibit a variable state of phase segregation after 18 months storage time at room temperature depending on thermal history. The experimental evidence for partial miscibility includes:

1. The observation of broad TSDC α peaks (thermal treatment A) and well-defined peaks near the glass transition temperature of PCL (thermal treatment B) except for the 80/20 PC/PCL blend.

2. The observation of two T_g's by DSC for samples with treatment B except for the 80/20 PC/PCL blend.

3. TEM micrographs reveal the existence of a PC-rich phase in a 20/80 PC/PCL isothermally crystallized sample.

4. The spherulitic growth rate of the PCL component is markedly slowed in freshly extruded samples as compared to the 18 months aged ones as the presence of PC chains in the miscible melt restrains the diffusion of the PCL chains to the crystallization front.

Once the blends have undergone phase separation, only extrusion in the melt or solution mixing can recover their miscibility. The driving force behind this segregation process seems to be the slow crystallization of the PCL component. Discrepancies with the Fox equation

whether it is applicable on the whole or partial composition range and with the models used by several authors to follow the compositional variation of the blends T_g might be the result of the dependence on the partial miscibility of the blends with aging, thermal treatment, and crystallinity degree.

Even though the miscibility observed by TSDC in the quenched samples is low as indicated by broad α modes, the local relaxations are affected by these concentration fluctuations. The profiles of the energy distributions (normalized to a unit area) deduced from DSA show that the secondary modes in the blends differ from that of the homopolymers. The highest energy components of the distribution are depleted while the low-energy Debye modes increase their contribution as the PC content increases. It is generally accepted that when broad secondary peaks are present there exists an increasing length in the reorienting entities responsible for the local modes. The rigidity of the neighboring PC chains interferes with the longest range motions which are still local but are closer to the cooperativity present in the α relaxation. The broad α modes observed in the quenched samples, except for the 20/80 PC/PCL blend, are indicative of composition fluctuations, resulting in reduced miscibility of the blend components as their crystallinity grows.

Additionally, the low intensity of the α, β, and γ peaks is interpreted as the result of the existence of a constrained amorphous PCL phase directly affected by the PC and PCL crystal lamellae.

The application of several experimental techniques that probe different aspects and different scales to the study of a blend system that was considered until now as miscible in the amorphous state has shown that storage time, thermal treatments, and development of crystallinity of both components can greatly influence the degree of miscibility.

Acknowledgment. Financial support from FONACIT, Venezuela (Projects G97-000594 and F95-000716), is gratefully acknowledged. The authors thank Dr. Marco Sabino for his collaboration in preparing the blend films.

References and Notes

(1) Cruz, C. A.; Paul, D. R.; Barlow, J. W. *J. Appl. Polym. Sci.* **1979**, *23*, 589.
(2) Jonza, J. M.; Porter, R. S. *Macromolecules* **1986**, *19*, 1946.
(3) Cheung, Y. W.; Stein, R. S.; Wignall, G. D.; Yang, H. E. *Macromolecules* **1993**, *26*, 5365.
(4) Cheung, Y. W.; Stein, R. S. *Macromolecules* **1994**, *27*, 2512.
(5) Cheung, Y. W.; Stein, R. S.; Lin, J. S.; Wignall, G. D. *Macromolecules* **1994**, *27*, 2520.
(6) Cheung, Y. W.; Stein, R. S. *Macromolecules* **1994**, *27*, 3589.
(7) Balsamo, V.; Calzadilla, N.; Mora, G.; Müller, A. J. *J. Polym. Sci., Part B: Polym. Phys.* **2001**, *39*, 771.
(8) Ketelaars, A. A. J.; Papantoniou, Y.; Nakayama, K. *J. Appl. Polym. Sci.* **1997**, *66*, 921.
(9) Lodge, T.; McLeish, T. C. B. *Macromolecules* **2000**, *33*, 5278.
(10) Chung, G.-C.; Kornfield, J. A.; Smith, S. D. *Macromolecules* **1994**, *27*, 5729.
(11) Cruz, C.; Paul, D. R.; Barlow, J. *Polym. Eng. Sci.* **1991**, *35*, 589.
(12) Cruz, C. A.; Barlow, J. W.; Paul, D. R. *Macromolecules* **1979**, *12*, 726.
(13) Utracki, L. *Polymer Alloys and Blends: Thermodynamics and Rheology*; Hanser Publishers: New York, 1989.
(14) Coleman, M. M.; Painter, P. C. *J. Appl. Spectrosc. Rev.* **1984**, *20*, 255.
(15) Hatzius, K.; Li, Y.; Werner, M.; Jungnickel, B. J. *Angew. Makromol. Chem.* **1996**, *243*, 177.
(16) Varnell, D. F.; Runt, J. P.; Coleman, M. M. *Macromolecules* **1981**, *14*, 1350.
(17) Kim, C. K.; Paul, D. R. *Polym. Eng. Sci.* **1994**, *34*, 24.
(18) Nishi, T.; Wang, T. T. *Macromolecules* **1975**, *8*, 909.
(19) Heijboer, J. *Int. J. Polym. Mater.* **1977,** *6*, 11.
(20) Shimizu, H.; Horiuchi, S.; Kitano, T. *Macromolecules* **1999**, *32*, 537.
(21) Georgoussis, G.; Kyritsis, A.: Bershtein, V. A.; Fainleib, A. M.; Pissis, P. *J. Polym. Sci., Part B: Polym. Phys.* **2000**, *38*, 3070.
(22) Katana, G.; Fischer, E. W.; Hack, T.; Abetz, V.; Kremer, F. *Macromolecules* **1995**, *28*, 2714.
(23) De Juana, R.; Hernández, R.; Peña, J. J.; Santamaría, A.; Cortázar, M. *Macromolecules* **1994**, *27*, 6980.
(24) Becker, O.; Simon, G. P.; Rieckmann, T.; Forsythe, J.; Rosu, R.; Völker, S.; O'Shea, M. *Polymer* **2001**, *42*, 1921.
(25) Vanderschueren, J.; Janssens, A.; Ladang, M.; Niezette, J. *Polymer* **1982**, *23*, 395.
(26) Laredo, E.; Grimau, M.; Müller, A.; Bello, A.; Suarez, N. *J. Polym. Sci., Part B: Polym. Phys.* **1996**, *34*, 2863.
(27) Aldana, M.; Laredo, E.; Bello, A.; Suarez, N. *J. Polym. Sci., Part B: Polym. Phys.* **1994**, *32*, 2197.
(28) Bello, A.; Laredo, E.; Grimau, M. *Phys. Rev. B* **1999**, *60*, 12764.
(29) Laredo, E.; Bello, A.; Hernández, M. C.; Grimau, M. *J. Appl. Phys.* **2001**, *90*, 5721.
(30) Bittiger, H.; Marchessault. R. H.; Niegisch, W. D. *Acta Crystallogr. B* **1970**, *26*, 1923.
(31) Bonart, R. *Makromol. Chem.* **1966**, *92*, 149.
(32) Hernández, M. C.; Laredo, E.; Grimau, M.; Bello, A. *Polymer* **2000,** *41*, 7223.
(33) Turi, E. A., Ed. *Thermal Characterization of Polymeric Materials*, 2nd ed.; Academic Press: San Diego, 1997; Vol. 1.
(34) Diaz-Calleja, R.; Sanchis, M. J.; Alvarez, C.; Riande, E. *J. Appl. Phys.* **1997**, *81*, 3685.
(35) Urakawa, O.; Fuse, Y.; Hori, H.; Tran-Cong, Q.; Yano, O. *Polymer* **2001**, *42*, 765.
(36) Huong, D. M.; Drechsler, M.; Cantow, H. J.; Möller, M. *Macromolecules* **1993**, *26*, 864.
(37) Li, Y.; Jungnickel, B. J. *Polymer* **1993**, *34*, 9.
(38) Nojima, S.; Kuroda, M.; Sasaki, S. *Polym. J.* **1997**, *29*, 642.
(39) Bashir, Z.; Hill, M. J.; Keller, A. *J. Mater. Sci. Lett.* **1986**, *5*, 876.
(40) Kressler, J.; Kammer, H. W.; Silvestre, C.; DiPace, E.; Cimmino, S.; Martuscelli, E. *Polym. Networks Blends* **1991**, *1*, 225.
(41) Wang, Z.; Wang, X.; Yu, D.; Jiang, B. *Polymer* **1997**, *38*, 23.
(42) Defieuw, G.; Groeninckx, G.; Reynaers, H. *Polym. Commun.* **1989**, *30*, 267.
(43) Ong, C. J.; Price, F. P. *J. Polym. Sci., Polym Symp.* **1978**, *63*, 45.

MA0204655